



Study Some Optical and Structural Properties of $Pb_{2-x}Sb_xBa_2Ca_2Cu_3O_{10}$ Thin Films Substitution with Antimony Prepare by Pulsed Laser Deposition Method

Jaafar S. Mohammed^{1*}, Ali H. Al Dulaimi², Haider Sahi Hussein³, Kareem A. Jasim⁴

Abstract

In this paper, a thin film of ($Pb_{2-x}Sb_xBa_2Ca_2Cu_3O_{10}$) was deposited on glass substrate using Pulsed Laser Deposition (PLD) method with a power of 400 watts, a frequency of 6 Hz and a rate of 200 pulses. The results showed that the X-ray measurements of the prepared films (crystals). Then, optical and compositional measurements were performed on the films to determine the transmittance and absorption spectrum as a function of the incident wavelength, the value and type of the energy gap. It was found that the energy gap decreases after annealing to become (1.9 eV). As for the structural measurements, the degree of crystallinity and the growth rate of granules and films with direct transfer were calculated. These results are close to those which are obtained previously. The thin films were thermally annealed at 400 °C for two hours. Thermal annealing greatly affects the prepared films, as the annealing improves the properties of the films.

51

Key Words: Thin Film, $Pb_{2-x}Sb_xBa_2Ca_2Cu_3O_{10}$, LPD, Thermal Annealing, Energy Gap.

DOI Number: 10.14704/nq.2022.20.2.NQ22024

NeuroQuantology 2022; 20(2):51-56

Introduction

Superconducting materials and their technologies have very great benefits nowadays in our lives. It contains significant improvements in efficiency, cost and performance in many modern industrial, medical, laboratory and technological devices such as medical devices, computers, energy meters and communications. In addition, the ability of superconducting materials to generate, transmit and store electrical energy; therefore, they are used as environmentally friendly energy transmission tools (Jasim K.A., T.M.A. and S.R., 2014) Superconductivity is a phenomenon based mainly

on quantum theory that some materials are exposed to when cooled to low temperatures. At the critical temperature, these materials allow a constant electric current to flow without loss due to zero resistance. Large and powerful super magnets are used in science, medicine, research and technology development (Kareem. A. Jasim, 2011). In addition, very low AC losses in superconductors may lead to significant energy savings in power applications (Jasim, K.A., 2012).

Corresponding author: Jaafar S. Mohammed

Address: ^{1*}Department of Physics, College of Science, University of Diyala, Iraq; ²Department of Physics, College of Science, University of Diyala, Iraq; ³General Directorate of Karbala Education, Karbala, Iraq; ⁴Department of Physics, College of Education for Pure Sciences Ibn Al-Haitham, University of Baghdad, Iraq.

Relevant conflicts of interest/financial disclosures: The authors declare that the research was conducted in the absence of any commercial or financial relationships that could be construed as a potential conflict of interest.

Received: 05 December 2021 **Accepted:** 08 January 2022



Since the manufacturing of the first laser system in the early 1960s, the areas of laser usage have been increased so that there is no longer a field where lasers have not entered, and researchers have been able to vaporize materials that are difficult to vaporize by other methods (Muslim Fadel & Heba Salam, 2009). The absorption process is very important for the laser interaction with the material to occur. This absorption process is a major source of energy within the material. (Kassim M. Wadi, Kareem A. Jasim, Auday H. Shaban, Mustafa K. Kamil, F.K.N., 2020). The laser beam emitted from the source determines what happens to the laser-radiated materials and the compound is a group of oxides, (R. Eason., 2007) which are copper oxide, barium oxide, calcium oxide and lead, which are among the most important materials that are used in photovoltaic applications. It is a cheap and non-toxic material. Copper oxide is dark brown to black odorless, barium oxide is white or yellow in color, and calcium oxide is white in color. Lead oxide is yellow and they are all used in solar energy applications, especially solar photovoltaic collectors, where these applications require high efficiency and good range.

In this work, a thin film of $Pb_{2-x}Sb_xBa_2Ca_2Cu_3O_{10}$ was deposited on glass substrate using Pulsed Laser Deposition (PLD) method with a power of 400 watts, a frequency of 6 Hz and a rate of 200 pulses was investigated the role of antimony (Sb) partial substitution of the $Pb_{2-x}Sb_xBa_2Ca_2Cu_3O_{10}$ compound, its effects on structural characterization (structure and surface morphology pattern), optical and compositional measurements. We investigate also the influence of antimony content on optical properties of $Pb_{2-x}Sb_xBa_2Ca_2Cu_3O_{10}$ in different concentrations of antimony to replace copper and their characterization.

Modeling and Working Methods

In this paper, the uncoated $Pb_{2-x}Sb_xBa_2Ca_2Cu_3O_{10}$ compound is substitute with antimony in different proportions. After samples were prepared, they were pressed into discs (1x1 cm) and deposited on a glass substrate with dimensions (7 cm * 2.5 cm) by using the evaporation technique. A pulsed YAG-Nd laser with a wavelength of 1.06 μ m (200) pulses, 400 watts, frequency 6 Hz, (Khalid. H. Razeg, 2017) manufactured by EPLS. (I. Fasaki, A. Giannoudakos, and M. Kompitsas, 2008). The system included (a bell made of Pyrex glass of 1mm

thickness, 320mm in diameter and 45 cm height) and a system consisting of a mechanical rotary pump to degas the bell. After X-ray examinations, the samples were annealed at 400°C. As in Figure (1).

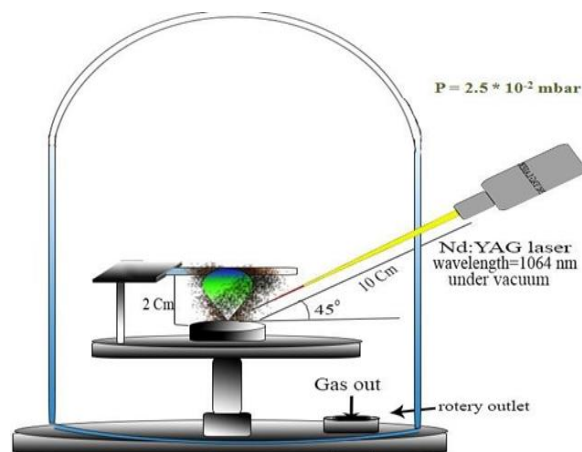


Figure 1. Illustration of the PLD system used in this work.

The working side includes the following measurements:

1. Structure Measurements: X-rays in order to identify the phase structures for membranes the X-ray diffraction device type (1840)PW Phillips (which works with X-rays with wavelength 1.5406Å from Cu-K α source (Heba S. Tareq, 2014) was used.
2. The study included optical measurements by calculating the optical properties of the thin films (through studying the transmittance and absorption spectra of the prepared films), whereas; the value of the energy gap was studied by using a UV/1800 spectrophotometer provided by (BIOTECH) company. After that, the thin films were thermally annealed using an electric furnace at 400°C for 2h.

52

Results and Discussion

1. Structural Properties

X-ray Diffraction

XRD was examined for $Pb_{2-x}Sb_xBa_2Ca_2Cu_3O_{10}$ Thin film polycrystalline samples with $x = 0, 0.1$ to 0.3 for deflection angle ranging from 10° to 80° , the results shown in Figures 2, 3, 4 and 5 indicated that all the samples have Polycrystalline structure. The pattern (XRD) illustration of $Pb_{2-x}Sb_xBa_2Ca_2Cu_3O_{10}$ Substitution by Sb shows that all samples contain a high percentage of the $Pb_{2-x}Sb_xBa_2Ca_2Cu_3O_{10}$ -phase

and a few low-intensity phase peaks with The emergence of some phases of impurity (Kamil, 2020) and (Mohammed A., Rihab N. Fadhil, Shatha H, Mahdie, Kareem A. Jasim, 2021) From X-ray diffraction, the degree of crystallinity and particle size of all the blocked films were calculated as shown (D.I. Rusu*, G.G. Rusu and D. Luca, 2011) and (Raghad S. Abbas i, 2021)

Table 1. Shows the values of Degree of crystallinity, Total area and crystal size computed from the Scherrer equation as a function of Sb concentration

Doping ratio	Pure	Sb=0.1	Sb=0.2	Sb=0.3
Degree of crystallinity	29.31%	30.30%	33.92%	33.39%
Total area	156515	142757	152128	158739
crystal size (nm)	12.5237	22.49946095	19.14549303	9.429800812

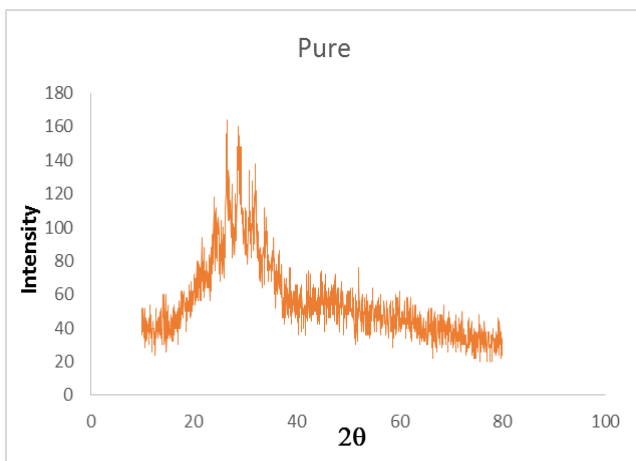


Figure 2. Deposition of XRD patterns of pure $Pb_2Ba_2Ca_2Cu_3O_{10}$ films on glass bases

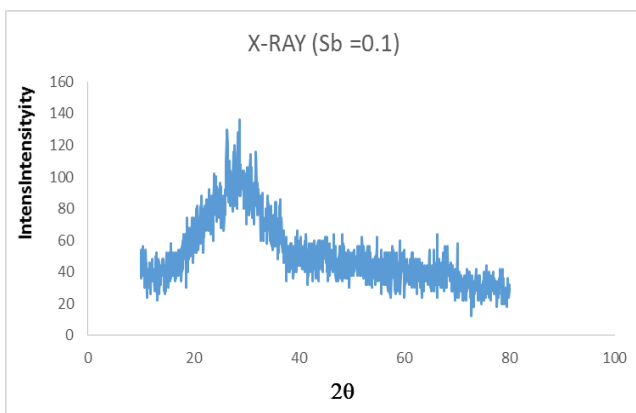


Figure 3. Deposition of XRD patterns of $Pb_{1.9}Sb_{0.1}Ba_2Ca_2Cu_3O_{10}$ films on glass bases

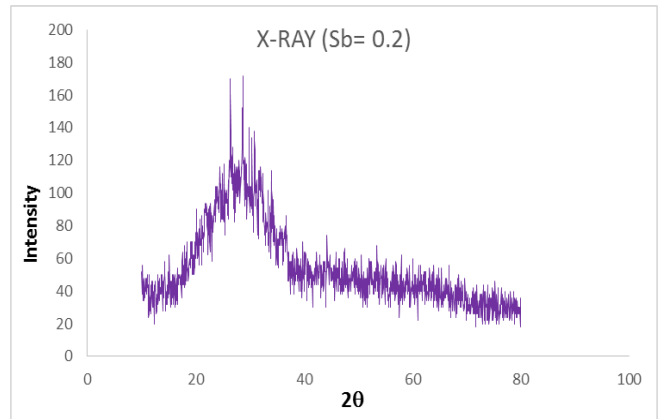


Figure 4. Deposition of XRD patterns of $Pb_{1.8}Sb_{0.2}Ba_2Ca_2Cu_3O_{10}$ films on glass bases Intensity

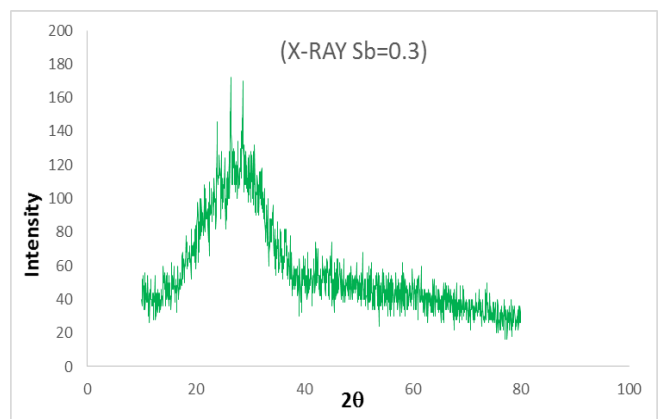


Figure 5. Deposition of XRD patterns of $Pb_{1.7}Sb_{0.3}Ba_2Ca_2Cu_3O_{10}$ films on glass bases

2. Optical Properties

Transmittance and Absorbance Spectrum

We notice a sudden increase in transmittance values with increasing the wavelength in the range of (300-700 nm), then the curve begins to stabilize for the wavelength more than 700 nm, which means that the oxide compound ($Pb_{2-x}Sb_xBa_2Ca_2Cu_3O_{10}$) has a higher transmittance for wavelengths greater than 700 nm. From Figures (6), (7) we note that its absorption curves behave exactly the opposite of its transmittance curves, especially after the annealing process. In Figure (8), (9) it is shown that the absorbance of the membrane ($Pb_{2-x}Sb_xBa_2Ca_2Cu_3O_{10}$) suddenly drops at wavelengths (300-700 nm) and then begins to stabilize after wavelengths greater than (700 nm).



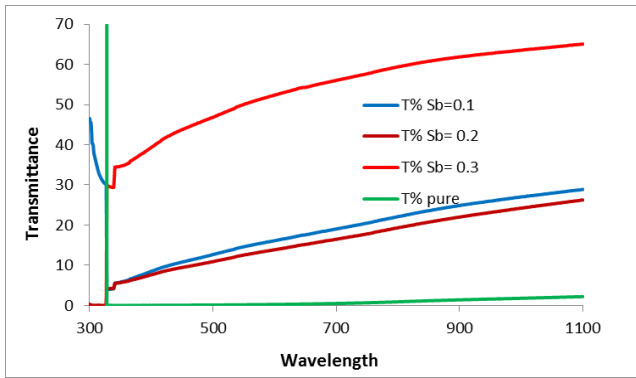


Figure 6. Transmittance as a function of wavelength before annealing of $Pb_{2-x}Sb_xBa_2Ca_2Cu_3O_{10}$ with different Sb concentration

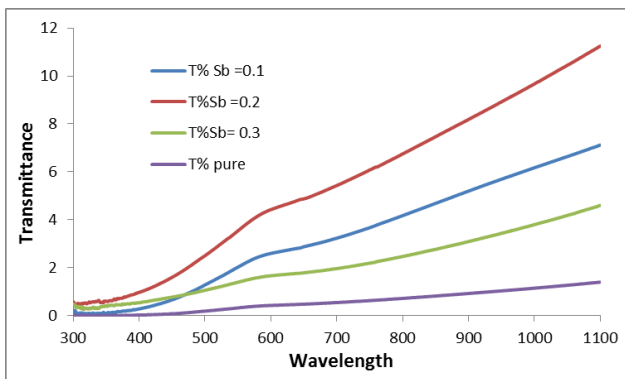


Figure 7. Transmittance as a function of wavelength after annealing of $Pb_{2-x}Sb_xBa_2Ca_2Cu_3O_{10}$ with different Sb concentration

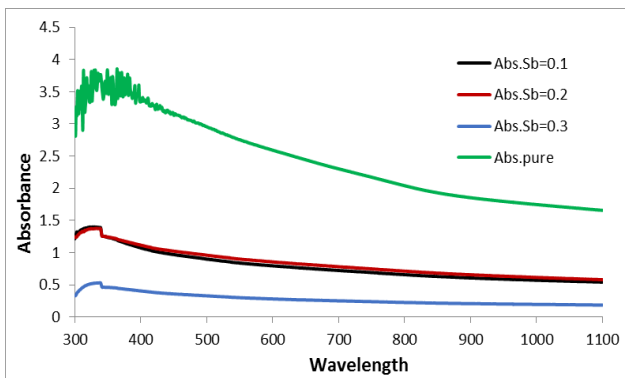


Figure 8. Absorbance as a function of wavelength before annealing of $Pb_{2-x}Sb_xBa_2Ca_2Cu_3O_{10}$ with different Sb concentration

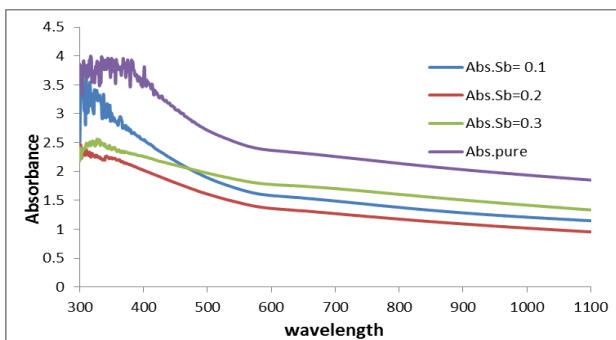


Figure 9. Absorbance as a function of wavelength after annealing of $Pb_{2-x}Sb_xBa_2Ca_2Cu_3O_{10}$ with different Sb concentration

The optical band gap was determined using the relationship $(\alpha h\nu = A (h\nu - E_g)^r)$, where α is the absorption coefficient, $h\nu$ is the photon energy, E_g is the optical bandgap, A is a constant that does not depend on the photon energy and r has four numerical values (1/2 direct permissible, 2 indirect allowed, 3 for direct forbidden and 3/ 2 for prohibited indirect optical transitions). (R.K. Puri, V.K. Babbar, (2001)) and it is determined by plotting $(\alpha h\nu)^2$ against the $h\nu$ curves, from the extrapolation of the linear region of the energies (J.Tauc, 1974). It is observed that the direct optical bandgap before annealing decreases by 2.5 to 2.1 eV, as shown in Figure 10(a, b, c, d). After performing the annealing process, we observe a decrease in the energy gap of the film ($Pb_{2-x}Ba_2Ca_2Cu_3O_{10} + x$) from (2.3 to 1.9 eV), as shown in Figure. 11(a, b, c, d) Table nomor(2) represents the values obtained from the research.

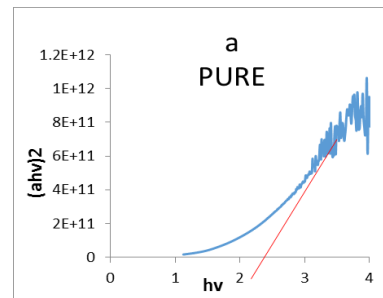


Figure 10(a). Energy gap of $Pb_{2-x}Sb_xBa_2Ca_2Cu_3O_{10}$ before annealing

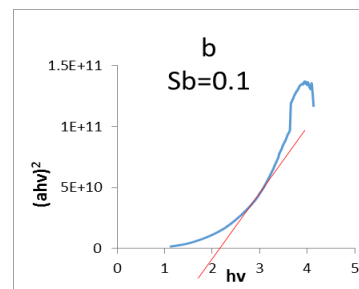


Figure 10(b). Energy gap of $Pb_{1.9}Sb_{0.1}Ba_2Ca_2Cu_3O_{10}$ before annealing (Sb=0.1)

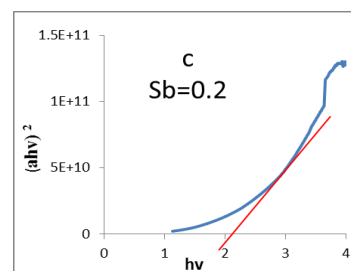


Figure 10(c). Energy gap of $Pb_{1.8}Sb_{0.2}Ba_2Ca_2Cu_3O_{10}$ before annealing (Sb=0.2)



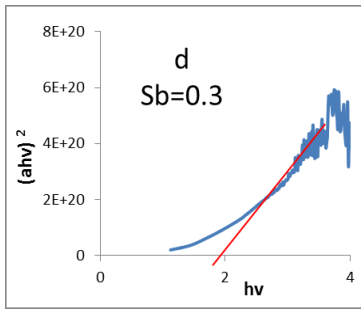


Figure 10(d). Energy gap of $Pb_{1.7}Sb_{0.7}Ba_2Ca_2Cu_3O_{10}$ before annealing (Sb=0.3)

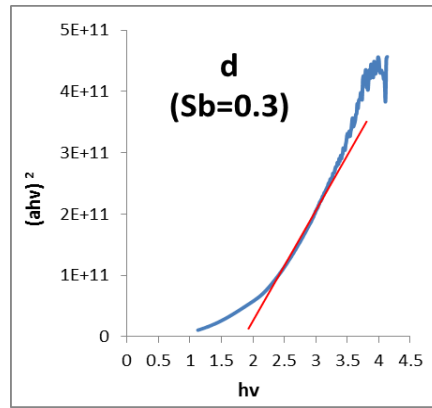


Figure 11(d). Energy gap of $Pb_{1.9}Sb_{0.9}Ba_2Ca_2Cu_3O_{10}$ after annealing (Sb=0.3)

After performing the annealing process, we observed a decrease in the energy gap of the film ($Pb_{2-x}Sb_xBa_2Ca_2Cu_3O_{10}$) from (2.3 to 1.9 eV) as shown in Figure 11(a, b, c, d) and Table (2) represents the values obtained from the research.

Table 2. Represents the values obtained from the research

Doping ratio	Pure (Ev)	Sb=0.1(Ev)	Sb=0.2(Ev)	Sb=0.3(Ev)
Energy gap before annealing eV	2.5	2.4	2.3	2.1
Energy gap after annealing (400 OC)	2.3	2.4	2.35	1.9

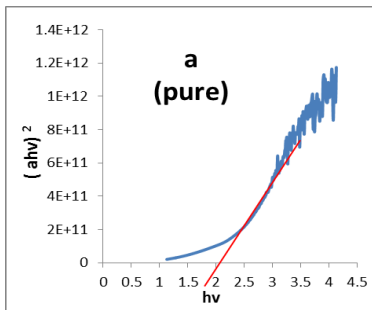


Figure 11(a). Energy gap of $Pb_{2-x}Sb_xBa_2Ca_2Cu_3O_{10}$ after annealing (pure)

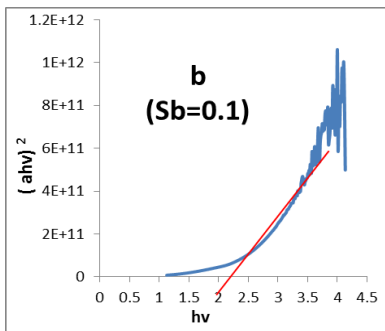


Figure 11(b). Energy gap of $Pb_{1.9}Sb_{0.9}Ba_2Ca_2Cu_3O_{10}$ after annealing (Sb=0.1)

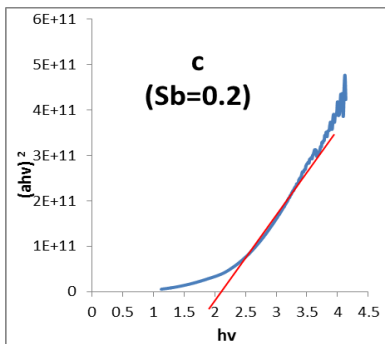


Figure 11(c). Energy gap of $Pb_{1.9}Sb_{0.9}Ba_2Ca_2Cu_3O_{10}$ after annealing (Sb=0.2)

Conclusion

From the results that we obtained, it was found that the $(Pb_{2-x}Ba_2Ca_2Cu_3O_{10+x})$ thin films ($Pb_{2-x}Sb_xBa_2Ca_2Cu_3O_{10}$) which were blocked by thermal laser evaporation method under the above preparation conditions, have a polycrystalline structure. From the calculation of the energy gap of the $(Pb_{2-x}Sb_xBa_2Ca_2Cu_3O_{10})$ film, we found that its value was (1.9 eV) after annealing. The effect of thermal annealing at 400°C on the energy gap value of $(Pb_{2-x}Sb_xBa_2Ca_2Cu_3O_{10})$. As the annealing temperature increased, the energy gap value decreased. Moreover, we found that the thermal annealing has increased Optical permeability of film $(Pb_{2-x}Sb_xBa_2Ca_2Cu_3O_{10})$.

References

Rusu DI, Rusu GG, Luca D. Structural Characteristics and Optical Properties of Thermally Oxidized Zinc Films. *Acta Physica Polonica A* 2011; 119(6): 850-856.

Tareq HS. Study the Effect of Rapid Thermal Annealing on Thin Films Prepared by Pulse Laser Deposition Method. *Journal of Engineering and Technology* 2014; 32(Part B): 444-452.

Stamatakis M, Tsamakis D, Brilis N, Fasaki I, Giannoudakos A, Kompitsas M. Hydrogen gas sensors based on PLD grown NiO thin film structures. *Physica status solidi (a)* 2008; 205(8): 2064-2068.

Tauc J. *Amorphous and Liquid Semiconductors*. London and New York: Plenum Press 1974.



- Jasim KA, Thejeel MA, Al-Khafaji RS. The Effect of Doping by Sr on the Structural, Mechanical and Electrical Characterization of $La_1Ba_{1-x}Sr_xCa_2Cu_4O_8$. $5+\delta$. *Ibn AL-Haitham Journal For Pure and Applied Science* 2017; 27(1): 170-175.
- Jasim KA. Superconducting properties of $Hg_{0.8}Cu_{0.15}Sb_{0.05}Ba_2Ca_2Cu_3O_{8+\delta}$ ceramic with controlling sintering conditions. *Journal of superconductivity and novel magnetism* 2012; 25(6): 1713-1717.
- Kamil MK, Jasim KA. Calculating of crystalline size, strain and Degree of crystallinity of the compound ($HgBa_2Ca_2Cu_3O_{8+\sigma}$) by different method. *In IOP Conference Series: Materials Science and Engineering* 2020: 928(7).
- Jasim KA, Alwan TJ, Al-Lamy HK, Mansour HL. Improvements of Superconducting Properties of $Hg_{0.6}Pb_{0.25}Sb_{0.15}Ba_2Ca_2Cu_3O_{8+\delta}$ Ceramic by controlling the sintering Time. *Journal of superconductivity and novel magnetism* 2011; 24(6): 1963-1966.
- Wadi KM, Jasim KA, Shaban AH, Kamil MK, Nsaif FK. The Effects of Sustainable Manufacturing Pressure on the Structural Properties of the $Pb_2Ba_2Ca_2Cu_3O_{9+\sigma}$ Compound. *Journal of Green Engineering (JGE)* 2020; 10(9): 6052-6062.
- Razeg KH, Al-Hilli MF, Khalefa AA, Aadim KA. Structural and Optical Properties of $(Li_xNi_{2-x}O_2)$ Thin Films Deposited by Pulsed Laser Deposited (PLD) Technique at Different Doping Ratio. *International Journal of Physics* 2017; 5(2): 46-52.
- Thejeel MAN, Fadhil RN, Mahdie SH, Jasim KA, Shaban AH. Effect of Partial Substitution of Sr by Ba on the Structural Properties of $Tl_{1-0.8}Ni_{0.2}Sr_{2-x}Br_xCa_2Cu_3O_{9-\delta}$ System. *In Key Engineering Materials* 2021; 900: 172-179.
- Fadel M, Salam H. Study Optical properties of copper oxide films Prepared by Laser. *University Science Magazine Al-Nahrain* 2009.
- Eason, R. (Ed.). (2007). *Pulsed laser deposition of thin films: applications-led growth of functional materials*. John Wiley & Sons.
- Puri RK, Babbar VK. *Solid State Physics and Electronics*, India: Chand and Company Ltd. 2001.
- Al-Khafaji RSA, Jasim KA. Dependence the microstructure specifications of earth metal lanthanum La substituted $Bi_2Ba_2CaCu_2-xLa_xO_8$ on cation vacancies. *AIMS Materials Science* 2021; 8(4): 550-559.
- Radhi AH, Du EAB, Khazaa FA, Abbas ZM, Aljelawi OH, Hamadan SD, Almashhadani HA, Kadhim MM. HOMO-LUMO energies and geometrical structures effecton corrosion inhibition for organic compounds predict by DFT and PM3 methods. *NeuroQuantology* 2020; 18(1): 37-45.

